

Gap Anisotropy in Layered Superconductors Due to Rashba and Dresselhaus Spin-Orbit Interactions

Bahruz Suleymanli

Physics Department, Yıldız Technical University, 34220 Esenler, Istanbul, Türkiye

B. Tanatar

Department of Physics, Bilkent University, 06800 Ankara, Türkiye

(Dated: December 25, 2024)

The theory of layered superconductors is extended in the presence of Rashba and Dresselhaus spin-orbit interactions (SOIs). Using the intralayer BCS-like pairing interaction and employing the Gor'kov formalism, we obtain analytical expressions for the temperature Green's functions and determine the gap function Δ which becomes complex in the presence of SOIs. In the absence of SOIs, Δ is isotropic at both zero and finite temperatures, but it becomes anisotropic even in the presence of a single SOI. This anisotropy is related to the extra $\cos k_z$ factors in which the k_z momentum along the z direction contributes to the magnitude of the gap function. It is also found that SOIs suppress Δ at both zero and finite temperatures, and for certain critical values of SOIs and beyond Δ vanishes. Analytical expressions for the critical values of SOIs at zero temperature are obtained. Additionally, how the BCS equation for layered superconductors changes in the presence of SOIs is determined.

I. INTRODUCTION

Rashba and Dresselhaus SOIs are foundational in the development of spintronic technologies due to their capacity to control spin dynamics via electric fields in systems lacking inversion symmetry [1–5]. The Rashba effect, with spin splitting linearly dependent on momentum, is prominent in structures with structural asymmetry, such as the Au(111) surface. This effect is observable through angle-resolved photoemission spectroscopy (ARPES), which highlights the alignment of electron spin with a momentum-dependent effective magnetic field, a feature advantageous for external manipulation via electric and magnetic fields [6, 7]. Conversely, Dresselhaus SOI arises from bulk inversion asymmetry in crystals, notably zinc-blende structures like GaAs, introducing cubic spin splitting terms [8]. These interactions are particularly useful in heterostructures, where controlled tuning can reduce spin relaxation, thereby supporting long-lived spin states for advanced spintronic devices [9–11]. Experimental studies on 2D transition metal dichalcogenides and complex heterostructures highlight precise control over spin splitting and spin textures, which has fueled advancements in high-performance spintronics [12, 13].

In superconductors, Rashba and Dresselhaus SOIs significantly alter spin dynamics and electronic structure, with profound implications for topological superconductivity [14, 15]. These interactions induce spin-split bands that can enhance superconductivity in noncentrosymmetric materials, creating conditions favorable for Majorana fermions and robust spin textures, which are critical for topological quantum computing [5, 16]. Specifically, the Rashba SOI facilitates topological phase transitions in the presence of a Zeeman field, augmenting nondegenerate spin structures such that conventional s-wave superconductivity can exhibit p-wave characteristics [17–19]. Experimental results on proximity-induced

superconductivity in topological insulators like HgTe and InSb nanowires have shown zero-bias conductance peaks, which are indicative of Majorana zero modes [20–22]. Significant experimental milestones include the observation of 4π -periodic Josephson supercurrent in HgTe and the demonstration of a robust superconducting gap in InAs nanowires with epitaxial Al coating, both environments conducive to Majorana phenomena [23, 24]. Additionally, atomic chains on Pb surfaces with strong SOI offer further experimental evidence of Majorana zero modes localized at chain edges, marking an essential step toward practical topological quantum computing [25].

Layered systems provide a distinct platform for studying Rashba-type SOI effects in atomic-layer superconductors [26–29]. A prominent example involves Rashba SOI on a Si(111)-($\sqrt{7} \times \sqrt{3}$)-In surface, where experiments revealed an in-plane upper critical magnetic field exceeding the Pauli limit by nearly three times at zero temperature [26]. This phenomenon, enabled by dynamic spin-momentum locking, was confirmed through in-situ electron transport measurements and density functional theory (DFT), highlighting the resilience of superconductivity under high magnetic fields. Such spin-momentum locking forces electron spins to flip at each scattering event, suppressing paramagnetic pair-breaking and preserving superconductivity. Furthermore, Rashba SOI has been shown to induce spin-splitting in materials like Ge(111)- β ($\sqrt{3} \times \sqrt{3}$)-Pb and Si(111)-($\sqrt{3} \times \sqrt{3}$)-TlPb, as observed through ARPES [27, 30]. In these systems, Rashba SOI-stabilized spin textures support unusual phenomena, such as spatially modulated superconducting order parameters, suggesting atomic-layer superconductors as ideal platforms for realizing unconventional superconductivity and exploring topological states.

Studies on a one-atom-layer Tl-Pb compound on Si(111) have demonstrated a large Rashba spin splitting (≈ 250 meV) and two-dimensional superconductivity

ity with a transition temperature of 2.25 K [31]. Observations from ARPES and transport measurements in this system reveal strong electron-phonon coupling and a Berezinskii-Kosterlitz-Thouless (BKT) transition, both of which reflect its two-dimensional superconducting nature. Here, Rashba SOI promotes mixed spin-singlet and spin-triplet pairing, with a potential for chiral p-wave topological superconducting states. Similar unconventional superconducting phases, such as complex-stripe (CS) and helical phases, have been observed in multilayer Pb films, where Rashba SOI induces spatially modulated order parameters, extending the exploration of topological superconductivity in systems lacking inversion symmetry [32].

The experimental studies mentioned above, along with ongoing experiments, emphasize the importance of analyzing Rashba and Dresselhaus SOI effects in layered superconductors. In this context, it is theoretically reasonable to model these superconductors as periodically arranged layers, where Cooper pairs can tunnel between the superconducting planes [33–37]. This approach also extends the analysis of these SOI effects to high-temperature superconducting crystals, where the strong anisotropy in both structural and physical properties makes the combined study of SOI and anisotropy effects particularly intriguing [38]. Notably, in almost all these crystals, an energy gap anisotropy has been observed experimentally, supporting the unique properties of high-temperature superconductors [39–46].

In this study, we extend the theory of layered superconductors to include the effects of Rashba and Dresselhaus SOIs. To this end, using the isotropic intralayer pairing interaction and employing the Gor'kov formalism, we derive the equations of motion incorporating temperature Green's functions for layered superconductors, starting from the Hamiltonian of the problem examined in Sec. II. In Sec. III, we obtain analytical expressions for the temperature Green's functions through Fourier transforms. These functions allow us to formulate the gap equation for the layered superconductors, as shown in Sec. IV. The results for zero and finite temperatures are provided in Secs. V and VI, respectively. Conclusions are given in Sec. VII where we also point out the relevance of our results to some recent experiments. Some technical details related to the calculations are presented in Appendices A, B, and C.

II. MODEL AND EQUATIONS OF MOTION

The starting point of our theory is the Hamiltonian in the second quantization formalism for layered superconductors

$$H = \sum_{j\sigma} \int d^2r \{H_0 + H_T + H_{\text{BCS}} + H_{\text{R}} + H_{\text{D}}\}, \quad (1)$$

which includes free-electron propagation within each layer

$$H_0 = -\psi_{j\sigma}^\dagger(\mathbf{r}) \frac{\nabla^2}{2m} \psi_{j\sigma}(\mathbf{r}), \quad (2)$$

tunneling of the electrons between the layers

$$H_T = \frac{J}{2} \left\{ \psi_{j\sigma}^\dagger(\mathbf{r}) \psi_{j+1,\sigma}(\mathbf{r}) + \text{H. c.} \right\}, \quad (3)$$

an intralayer BCS-type pairing interaction

$$H_{\text{BCS}} = \frac{\lambda}{2} \psi_{j\sigma}^\dagger(\mathbf{r}) \psi_{j,-\sigma}^\dagger(\mathbf{r}) \psi_{j,-\sigma}(\mathbf{r}) \psi_{j\sigma}(\mathbf{r}), \quad (4)$$

and the effects of the Rashba

$$H_{\text{R}} = \alpha \sum_{\gamma} \psi_{j\gamma}^\dagger(\mathbf{r}) \left\{ (\sigma_x)_{\gamma\sigma} p_y - (\sigma_y)_{\gamma\sigma} p_x \right\} \psi_{j\sigma}(\mathbf{r}) \quad (5)$$

and Dresselhaus SOIs

$$H_{\text{D}} = \beta \sum_{\gamma} \psi_{j\gamma}^\dagger(\mathbf{r}) \left\{ (\sigma_x)_{\gamma\sigma} p_x - (\sigma_y)_{\gamma\sigma} p_y \right\} \psi_{j\sigma}(\mathbf{r}). \quad (6)$$

In the above, $\psi_{j\sigma}(\mathbf{r})$ and $\psi_{j\sigma}^\dagger(\mathbf{r})$ are the field operators in second quantization associated with an electron with spin σ at position \mathbf{r} in the j th layer, J is the tunneling energy, λ is the coupling constant of the BCS-type electron-electron interaction, α and β are the strengths of the Rashba and Dresselhaus SOI, respectively, γ is the spin index taking values \uparrow and \downarrow , and $\sigma_{x,y}$ are the Pauli matrices in spin space. We note that the interlayer distance is uniformly set to 1. Additionally, in all our calculations, we use a system of units in which both Planck's constant \hbar and Boltzmann's constant k_B are equal to 1.

By writing the Heisenberg representation of the field operator $\psi_{j\sigma}(\mathbf{r})$ as $\psi_{j\sigma}(\mathbf{r}, \tau) = e^{(H-\mu N)\tau} \psi_{j\sigma}(\mathbf{r}) e^{-(H-\mu N)\tau}$ in the equation of motion

$$\frac{\partial}{\partial \tau} \psi_{j\sigma}(\mathbf{r}, \tau) = [H - \mu N, \psi_{j\sigma}(\mathbf{r}, \tau)], \quad (7)$$

where H is the Hamiltonian given by Eq. (1) and μ is the chemical potential with $N = \int d^2r \psi_{j\sigma}^\dagger(\mathbf{r}) \psi_{j\sigma}(\mathbf{r})$ being the number of particles, and defining the temperature Green's functions

$$G_{jj'}^{ab}(\mathbf{r}, \tau; \mathbf{r}', \tau') = - \left\langle T_{\tau} \left(\psi_{ja}(\mathbf{r}, \tau) \psi_{j'b}^\dagger(\mathbf{r}', \tau') \right) \right\rangle, \quad (8a)$$

$$F_{jj'}^{ab}(\mathbf{r}, \tau; \mathbf{r}', \tau') = \left\langle T_{\tau} \left(\psi_{ja}(\mathbf{r}, \tau) \psi_{j'b}(\mathbf{r}', \tau') \right) \right\rangle, \quad (8b)$$

$$F_{jj'}^{\dagger ab}(\mathbf{r}, \tau; \mathbf{r}', \tau') = \left\langle T_{\tau} \left(\psi_{jb}^\dagger(\mathbf{r}, \tau) \psi_{j'a}^\dagger(\mathbf{r}', \tau') \right) \right\rangle, \quad (8c)$$

where Eqs. (8b) and (8c) define the case with $a = -b$, and guided by the anticommutation relations of the field operators we can find the following equation of motion containing the Green's functions defined in Eqs. (8a) – (8c)

$$\begin{aligned}
& \left[-\frac{\partial}{\partial \tau} + \frac{\nabla^2}{2m} + \mu \right] G_{jj'}^{ab}(\mathbf{r}, \tau; \mathbf{r}', \tau') - \frac{J}{2} \{ G_{j+1, j'}^{ab}(\mathbf{r}, \tau; \mathbf{r}', \tau') + G_{j-1, j'}^{ab}(\mathbf{r}, \tau; \mathbf{r}', \tau') \} \\
& + \lambda \sum_{\gamma} \left\{ G_{jj}^{a\gamma}(0+) G_{jj'}^{\gamma b}(\mathbf{r}, \tau; \mathbf{r}', \tau') - G_{jj}^{\gamma\gamma}(0+) G_{jj'}^{ab}(\mathbf{r}, \tau; \mathbf{r}', \tau') - F_{jj}^{a\gamma}(0+) F_{jj'}^{\dagger\gamma b}(\mathbf{r}, \tau; \mathbf{r}', \tau') \right\} \\
& - \sum_{\gamma} \left\{ \alpha \left((\sigma_x)_{a\gamma} p_y - (\sigma_y)_{a\gamma} p_x \right) + \beta \left((\sigma_x)_{a\gamma} p_x - (\sigma_y)_{a\gamma} p_y \right) \right\} G_{jj'}^{\gamma b}(\mathbf{r}, \tau; \mathbf{r}', \tau') \\
& = \delta_{jj'} \delta_{ab} \delta(\mathbf{r} - \mathbf{r}') \delta(\tau - \tau'). \tag{9}
\end{aligned}$$

When we follow a similar procedure to write Eq. (7) for

$\psi_{j\sigma}^{\dagger}(\mathbf{r}, \tau)$, we find another equation of motion as follows

$$\begin{aligned}
& \left[\frac{\partial}{\partial \tau} + \frac{\nabla^2}{2m} + \mu \right] F_{jj'}^{\dagger ab}(\mathbf{r}, \tau; \mathbf{r}', \tau') - \frac{J}{2} \{ F_{j+1, j'}^{\dagger ab}(\mathbf{r}, \tau; \mathbf{r}', \tau') + F_{j-1, j'}^{\dagger ab}(\mathbf{r}, \tau; \mathbf{r}', \tau') \} \\
& + \lambda \sum_{\gamma} \left\{ F_{jj}^{\dagger a\gamma}(0+) G_{jj'}^{\gamma b}(\mathbf{r}, \tau; \mathbf{r}', \tau') - G_{jj}^{\gamma\gamma}(0+) F_{jj'}^{\dagger ab}(\mathbf{r}, \tau; \mathbf{r}', \tau') + G_{jj}^{\gamma a}(0+) F_{jj'}^{\dagger\gamma b}(\mathbf{r}, \tau; \mathbf{r}', \tau') \right\} \\
& - \sum_{\gamma} \left\{ \alpha \left((\sigma_x)_{a\gamma} p_y - (\sigma_y)_{a\gamma} p_x \right) + \beta \left((\sigma_x)_{a\gamma} p_x - (\sigma_y)_{a\gamma} p_y \right) \right\} F_{jj'}^{\dagger\gamma b}(\mathbf{r}, \tau; \mathbf{r}', \tau') \\
& = 0. \tag{10}
\end{aligned}$$

Eqs. (9) and (10) are the equations of motion for the temperature Green's functions (8a) – (8c) in the presence of Rashba and Dresselhaus SOIs in layered superconductors. Note that in the case of $J = \alpha = \beta = 0$, we can find the equations of motion for pure superconductors without SOIs [47] from Eqs. (9) and (10)

$$\begin{aligned}
& \left[-\frac{\partial}{\partial \tau} + \frac{\nabla^2}{2m} + \mu \right] G_0(\mathbf{r}, \tau; \mathbf{r}', \tau') + \Delta_0 F_0^{\dagger}(\mathbf{r}, \tau; \mathbf{r}', \tau') \\
& = \delta(\mathbf{r} - \mathbf{r}') \delta(\tau - \tau'), \tag{11a}
\end{aligned}$$

$$\begin{aligned}
& \left[\frac{\partial}{\partial \tau} + \frac{\nabla^2}{2m} + \mu \right] F_0^{\dagger}(\mathbf{r}, \tau; \mathbf{r}', \tau') - \Delta_0^* G_0(\mathbf{r}, \tau; \mathbf{r}', \tau') = 0, \tag{11b}
\end{aligned}$$

where

$$\Delta_0 = |\lambda| F_0(0+), \quad \Delta_0^* = |\lambda| F_0^{\dagger}(0+), \tag{12}$$

and $\lambda = -|\lambda|$.

III. GREEN'S FUNCTIONS

Eqs. (9) and (10) allow us to find analytical expressions for the temperature Green's functions in layered superconductors in the presence of Rashba and Dresselhaus SOIs. To achieve this, we perform the following Fourier transforms in Eqs. (9) and (10)

$$\begin{aligned}
G_{jj'}^{ab}(\mathbf{r}, \tau; \mathbf{r}', \tau') &= T \sum_n \int_{-\pi}^{\pi} \frac{dk_z}{2\pi} \int_{-\infty}^{\infty} \frac{d^2k}{(2\pi)^2} \\
& e^{-i\omega_n(\tau - \tau')} e^{-ik_z(j - j')} e^{-i\mathbf{k}(\mathbf{r} - \mathbf{r}')} \\
& G^{ab}(\mathbf{k}, k_z, \omega_n), \tag{13a}
\end{aligned}$$

$$\begin{aligned}
F_{jj'}^{\dagger ab}(\mathbf{r}, \tau; \mathbf{r}', \tau') &= T \sum_n \int_{-\pi}^{\pi} \frac{dk_z}{2\pi} \int_{-\infty}^{\infty} \frac{d^2k}{(2\pi)^2} \\
& e^{-i\omega_n(\tau - \tau')} e^{-ik_z(j - j')} e^{-i\mathbf{k}(\mathbf{r} - \mathbf{r}')} \\
& F^{\dagger ab}(\mathbf{k}, k_z, \omega_n), \tag{13b}
\end{aligned}$$

where the Matsubara frequencies $\omega_n = (2n + 1)\pi T$ guarantee the proper Fermi statistics. Straightforward calculations shown in Appendix A demonstrate that by writing Eqs. (13a) and (13b) in the equations of motion (9) and (10), we find the following analytical functions for the temperature Green's functions in the presence of Rashba and Dresselhaus SOIs.

$$\begin{aligned}
G^{\uparrow\uparrow}(\mathbf{k}, k_z, \omega_n) &= G^{\downarrow\downarrow}(\mathbf{k}, k_z, \omega_n) \\
&= \frac{\omega_n^2 + \xi_{\mathbf{k}k_z}^2}{g}, \tag{14a}
\end{aligned}$$

$$\begin{aligned}
G^{\uparrow\downarrow}(\mathbf{k}, k_z, \omega_n) &= (G^{\downarrow\uparrow}(\mathbf{k}, k_z, \omega_n))^* \\
&= -\frac{i\omega_n + \xi_{\mathbf{k}k_z}}{g} \\
&\times \{ \alpha(k_y + ik_x) + \beta(k_x + ik_y) \}, \tag{14b}
\end{aligned}$$

$$\begin{aligned}
F^{\dagger\uparrow\downarrow}(\mathbf{k}, k_z, \omega_n) &= -F^{\dagger\downarrow\uparrow}(\mathbf{k}, k_z, \omega_n) \\
&= \frac{i\omega_n - \xi_{\mathbf{k}k_z}}{g} \Delta^*, \tag{14c}
\end{aligned}$$

where

$$g = (i\omega_n - \xi_{\mathbf{k}k_z}) (\omega_n^2 + \xi_{\mathbf{k}k_z}^2 + |\Delta|^2) + (i\omega_n + \xi_{\mathbf{k}k_z}) \xi_{SO}^2, \tag{15a}$$

$$\xi_{\mathbf{k}k_z} = \frac{\mathbf{k}^2}{2m} + J \cos k_z - \mu, \quad (15b)$$

$$\xi_{SO} = \pm \sqrt{(\alpha^2 + \beta^2)(k_x^2 + k_y^2) + 4\alpha\beta k_x k_y}, \quad (15c)$$

and

$$\Delta = |\lambda| F_{jj}^{\downarrow\uparrow}(0+), \quad \Delta^* = |\lambda| F_{jj}^{\uparrow\downarrow}(0+), \quad (16)$$

with $\lambda = -|\lambda|$. It should be noted that the ξ_{SO} determined by Eq. (15c) are the eigenenergies of the single-particle Hamiltonian $H_0 + H_R + H_D$ for a two-dimensional electron gas in the presence of Rashba and Dresselhaus SOIs [48]. We can see from Eqs. (14a) – (14c) that one of the main effects of Rashba and Dresselhaus SOIs on the Green's functions is through the function g , shown in Eq. (15a). Another notable effect is that while the normal Green's function components $G^{\uparrow\downarrow}$ and $G^{\downarrow\uparrow}$ are zero when $\alpha = \beta = 0$, they become non-zero when $\alpha \neq 0$ and/or $\beta \neq 0$. Note also that in the case of $J = \alpha = \beta = 0$, we can find the solutions of Eqs. (11a) and (11b) from Eqs. (14a) – (14c)

$$G_0(\mathbf{k}, \omega_n) = -\frac{i\omega_n + \xi_{\mathbf{k}}}{\omega_n^2 + \xi_{\mathbf{k}}^2 + \Delta_0^2}, \quad (17a)$$

$$F_0^\dagger(\mathbf{k}, \omega_n) = \frac{\Delta_0^*}{\omega_n^2 + \xi_{\mathbf{k}}^2 + \Delta_0^2}, \quad (17b)$$

where $\xi_{\mathbf{k}} = \frac{\mathbf{k}^2}{2m} - \mu$. It is also worth noting that for the case $J \neq 0$ and $\alpha = \beta = 0$, the results are also the same as in Eqs. (17a) and (17b), with the exception that $\xi_{\mathbf{k}}$ is replaced by $\xi_{\mathbf{k}k_z}$ in Eqs. (17a) and (17b).

It is important to emphasize that as seen from Eq. (17b), since the anomalous Green's functions $F_0(\mathbf{k}, \omega_n)$ and $F_0^\dagger(\mathbf{k}, \omega_n)$ are equal, the quantity Δ_0 determined by the equations in Eq. (12) is also real. Therefore, in Eqs. (17a) and (17b), it suffices to write the square of Δ_0 rather than its absolute value. However, as seen from Eq. (14c), when $\alpha \neq 0$ and/or $\beta \neq 0$, this equality does not hold, and Δ is not a real function. In other words, the presence of SOIs makes the Δ gap a complex function.

IV. GAP EQUATION

In this section, we examine the effects of Rashba and Dresselhaus SOIs on the gap equation. To do this, we rewrite Eq. (16) for Δ^* using Eq. (13b)

$$\Delta^* = |\lambda| T \sum_n \int_{-\pi}^{\pi} \frac{dk_z}{2\pi} \int_{-\infty}^{\infty} \frac{d^2k}{(2\pi)^2} F^{\uparrow\downarrow}(\mathbf{k}, k_z, \omega_n). \quad (18)$$

By substituting Eq. (14c) into Eq. (18), we obtain the following gap equation

$$1 = |\lambda| T \sum_n \int_{-\pi}^{\pi} \frac{dk_z}{2\pi} \int_{-\infty}^{\infty} \frac{d^2k}{(2\pi)^2} \frac{i\omega_n - \xi_{\mathbf{k}k_z}}{g}. \quad (19)$$

Eq. (19) shows that the effects of Rashba and Dresselhaus SOIs on the Δ gap function determined by Eq. (16) are analogous. If we consider the effect of only one SOI, whether it is Rashba or Dresselhaus, the same result for Δ is obtained in both cases. In the case of two SOIs, as seen from Eq. (15c), if the values of α and β are such that, for example, $\alpha = \alpha_0$ and $\beta = \beta_0$, and then they are swapped, i.e., $\alpha = \beta_0$ and $\beta = \alpha_0$, Δ remains unchanged. If we consider this equivalent form of Eq. (15a)

$$g = (i\omega_n - \xi_{\mathbf{k}k_z}) (\omega_n^2 + \xi_{\mathbf{k}k_z}^2 + |\Delta|^2 + \xi_{SO}^2) \times \frac{1}{1 - \frac{1}{(i\omega_n - \xi_{\mathbf{k}k_z}) \frac{\omega_n^2 + \xi_{\mathbf{k}k_z}^2 + |\Delta|^2 + \xi_{SO}^2}{2\xi_{SO}^2 \xi_{\mathbf{k}k_z}}}}, \quad (20)$$

by writing Eq. (20) in Eq. (19), we can express the gap equation as follows

$$1 = \sum_{\nu=0}^{\infty} I_{\nu}, \quad (21)$$

where

$$I_{\nu} = \frac{|\lambda| T}{2} \sum_n \int_{-\pi}^{\pi} \frac{dk_z}{2\pi} \int_{-\infty}^{\infty} \frac{d^2k}{(2\pi)^2} \frac{1}{\omega_n^2 + \xi_{\mathbf{k}k_z}^2 + |\Delta|^2 + \xi_{SO}^2} \times \left(\frac{1}{\left((i\omega_n - \xi_{\mathbf{k}k_z}) \frac{\omega_n^2 + \xi_{\mathbf{k}k_z}^2 + |\Delta|^2 + \xi_{SO}^2}{2\xi_{SO}^2 \xi_{\mathbf{k}k_z}} \right)^{\nu}} + \frac{1}{\left((-i\omega_n - \xi_{\mathbf{k}k_z}) \frac{\omega_n^2 + \xi_{\mathbf{k}k_z}^2 + |\Delta|^2 + \xi_{SO}^2}{2\xi_{SO}^2 \xi_{\mathbf{k}k_z}} \right)^{\nu}} \right). \quad (22)$$

It is important to emphasize that when writing Eqs. (21) and (22), the inequality

$$\left| (\pm i\omega_n - \xi_{\mathbf{k}k_z}) \frac{\omega_n^2 + \xi_{\mathbf{k}k_z}^2 + |\Delta|^2 + \xi_{SO}^2}{2\xi_{SO}^2 \xi_{\mathbf{k}k_z}} \right| > 1 \quad (23)$$

assumed to hold for each value of n, \mathbf{k} , and k_z . To show the validity of this, we rewrite the inequality (23) as follows

$$\frac{\omega_n^2 + \xi_{\mathbf{k}k_z}^2 + |\Delta|^2}{\xi_{SO}^2} > \frac{2}{\sqrt{1 + \frac{\omega_n^2}{\xi_{\mathbf{k}k_z}^2}}} - 1. \quad (24)$$

As seen, the left side of the inequality (24) is always positive. Therefore, the inequality (24) is always valid when $\omega_n^2 \geq 3\xi_{\mathbf{k}k_z}^2$, since in this case, the right side of inequality (24) is less than or equal to zero. For $0 < \omega_n^2 < 3\xi_{\mathbf{k}k_z}^2$, the inequality (24) leads to $\xi_{\mathbf{k}k_z}^2 + |\Delta|^2 > c \cdot \xi_{SO}^2$, where $0 < c < 1$. The left side of this final inequality corresponds to the excitation spectrum of layered superconductors without SOIs. Given that the addition to this spectrum from SOIs, scaled by a factor c less than 1, will

not exceed the spectrum, it is concluded that the inequality (24) also holds for the range $0 < \omega_n^2 < 3\xi_{\mathbf{k}k_z}^2$. Thus, it is found that the inequality (23) is valid for all values.

The inequality (23), we have just proven, also demonstrates that the integral I_0 has the largest integrand among the integrals in (22). Our calculations have also shown that the I_0 integral is significantly larger than the other I_ν integrals for $\nu \geq 1$. For instance, the computations in Appendix B reveal that the contribution of the I_1 integral to the results provided by the I_0 integral is exceedingly small. Therefore, we neglect the contribution of the I_1 integral in our calculations. Additionally, the integrands of the integrals I_2, I_3 , etc., are even smaller than I_1 , allowing us to neglect their contributions as well. Therefore, in our calculations, we focus on the integral I_0 , which provides the most significant contribution to the gap equation (21) in the presence of SOIs, and we assume $I_0 = 1$. In other words,

$$1 = |\lambda|T \sum_n \int_{-\pi}^{\pi} \frac{dk_z}{2\pi} \int_{-\infty}^{\infty} \frac{d^2k}{(2\pi)^2} \frac{1}{\omega_n^2 + \xi_{\mathbf{k}k_z}^2 + |\Delta|^2 + \xi_{SO}^2}. \quad (25)$$

Note that from Eq. (25), we can also derive the exact gap equation for the case without SOIs [47] by setting $\xi_{SO} = 0$.

Finally, we perform the summation over n . We know that a function like $\sum_{n=-\infty}^{\infty} f(n+1/2)$ can be expressed as the sum of residues of $\pi \tan \pi z f(z)$ at all the poles of $f(z)$, where $n+1/2 = z$ [49]. The poles of the function $f(z) = 1/(\omega_n^2 + \xi_{\mathbf{k}k_z}^2 + |\Delta|^2 + \xi_{SO}^2)$ are $z_{1,2} = \pm i\sqrt{\xi_{\mathbf{k}k_z}^2 + |\Delta|^2 + \xi_{SO}^2}/2\pi T$. Then, we can write the Eq. (25) as follows

$$1 = \frac{|\lambda|}{2} \int_{-\pi}^{\pi} \frac{dk_z}{2\pi} \int_{-\infty}^{\infty} \frac{d^2k}{(2\pi)^2} \frac{\tanh\left(\frac{\sqrt{\xi_{\mathbf{k}k_z}^2 + |\Delta|^2 + \xi_{SO}^2}}{2T}\right)}{\sqrt{\xi_{\mathbf{k}k_z}^2 + |\Delta|^2 + \xi_{SO}^2}}. \quad (26)$$

V. ZERO TEMPERATURE RESULTS

As noted earlier, in the cases where $\alpha \neq 0$ and/or $\beta \neq 0$, Δ is a complex function because $F^{\downarrow\uparrow} \neq F^{\uparrow\downarrow}$ in Eq. (16). Therefore, the main focus of our calculations

$$1 = -|\lambda|\rho_0^{2D} \int_{-\pi}^{\pi} \frac{dk_z}{2\pi} \ln \left(\frac{\sqrt{|\Delta|^2 + 2m(\mu - J \cos k_z)(\alpha + \beta)^2} + \sqrt{|\Delta|^2 + 2m(\mu - J \cos k_z)(\alpha - \beta)^2}}{4\omega_D} \right), \quad (31)$$

where $\rho_0^{2D} = m/2\pi$.

will be on how the magnitude of Δ changes with the presence of SOIs. For this purpose, we first examine how the magnitude $|\Delta|$ changes at zero temperature under the influence of Rashba and Dresselhaus SOIs. Knowing that in this limit $\tanh\left(\frac{\sqrt{\xi_{\mathbf{k}k_z}^2 + |\Delta|^2 + \xi_{SO}^2}}{2T}\right) \rightarrow 1$, if we switch to polar coordinates in \mathbf{k} space, we obtain the following integral from Eq. (26)

$$1 = \frac{|\lambda|m}{2} \int_{-\pi}^{\pi} \frac{dk_z}{2\pi} \int_{-\pi}^{\pi} \frac{d\theta}{2\pi} \int_{-\omega_D}^{\omega_D} \frac{d\epsilon}{2\pi} \frac{1}{\sqrt{\epsilon^2 + 2\eta_1\epsilon + \eta_2}}, \quad (27)$$

where

$$\epsilon = \frac{k_F}{m}(k - k_F), \quad (28a)$$

$$\eta_1 = J \cos k_z + m(\alpha^2 + \beta^2 + 2\alpha\beta \sin 2\theta), \quad (28b)$$

$$\eta_2 = |\Delta|^2 + J^2 \cos^2 k_z + 2m\mu(\alpha^2 + \beta^2 + 2\alpha\beta \sin 2\theta). \quad (28c)$$

It is important to note here that to avoid divergence in the integral of Eq. (26), a cutoff is introduced. This cutoff is based on the condition that in the current model, only electrons within an energy range of $2\omega_D$ around the Fermi surface are involved in the interaction. If we integrate Eq. (27) with respect to ϵ within these cutoff limits, we obtain

$$1 = -\frac{|\lambda|m}{2(2\pi)} \int_{-\pi}^{\pi} \frac{dk_z}{2\pi} \int_{-\pi}^{\pi} \frac{d\theta}{2\pi} \ln \left(\frac{\eta_3 + \eta_4 \sin 2\theta}{4\omega_D^2} \right), \quad (29)$$

where

$$\eta_3 = |\Delta|^2 + 2m(\alpha^2 + \beta^2)(\mu - J \cos k_z), \quad (30a)$$

$$\eta_4 = 4m\alpha\beta(\mu - J \cos k_z). \quad (30b)$$

Eq. (29) shows that at $T = 0$, the contribution of J to the gap function occurs only in the presence of a SOI.

By substituting Eq. (C6), calculated in Appendix C, into Eq. (29) and performing some routine calculations, we find that the gap equation depends solely on the integral with respect to k_z

A. Anisotropic gap function

Our model is based on intralayer pairing interaction. For such a system, in the absence of SOIs, the gap is

isotropic [35, 36, 50]. From Eq. (31), we observe that the presence of Rashba and Dresselhaus SOIs, or even just one of them, makes the gap function anisotropic. This anisotropy is related to the extra $\cos k_z$ factors that the

k_z momentum along the z direction contributes to the magnitude of the gap function. To illustrate this, let's find $|\Delta(k_z)|^2$ from Eq. (31) without integrating along k_z

$$|\Delta(k_z)|^2 = \Delta_0^2 - 2m\mu(\alpha^2 + \beta^2) + \frac{4m^2\mu^2\alpha^2\beta^2}{\Delta_0^2} + 2\left(m(\alpha^2 + \beta^2) - \frac{4m^2\mu\alpha^2\beta^2}{\Delta_0^2}\right)J\cos k_z + \frac{4m^2\alpha^2\beta^2}{\Delta_0^2}J^2\cos^2 k_z, \quad (32)$$

where $\Delta_0 = 2\omega_D e^{-\frac{1}{|\lambda|\rho_0^{2D}}}$. As seen from Eq. (32), when both SOIs are zero, $\Delta = \Delta_0$ and the gap is isotropic. In the presence of one SOI, the anisotropy in $|\Delta(k_z)|^2$ arises from the $\cos k_z$ term, and in the presence of both SOIs, the $\cos^2 k_z$ term also contributes to the anisotropy. This anisotropy is illustrated in Fig. 1 with the following dimensionless parameters.

$$|\tilde{\Delta}| = \frac{\Delta}{\Delta_0}; \tilde{J} = \frac{J}{\Delta_0}; \tilde{\mu} = \frac{\mu}{\Delta_0}; \tilde{\alpha} = \sqrt{\frac{m}{\Delta_0}}\alpha; \tilde{\beta} = \sqrt{\frac{m}{\Delta_0}}\beta. \quad (33)$$

In Eq. (32), as J increases for fixed values of α and β , $|\Delta|$ also increases. This indicates that electron tunneling between the layers enhances the anisotropic intralayer pairing interaction in the presence of SOI. When $k_z = 0$ and $\mu = J$, Δ equals Δ_0 . This scenario is depicted in Fig. 1, where all curves intersect at the point $\Delta = \Delta_0$. In contrast to J , larger values of SOIs suppress $|\Delta|$. If we consider $\alpha \neq 0$ and $\beta = 0$, then at $k_z = \pm\pi$, if $\alpha = \Delta_0/\sqrt{2m(\mu + J)}$, Δ becomes zero. This is illustrated by the dashed curve in Fig. 1. For values of α greater than this threshold, Δ takes values in a narrower range of k_z within $(-\pi, \pi)$, as shown by the dotted curve in Fig. 1. A similar pattern is observed when both $\alpha \neq 0$ and $\beta \neq 0$, with the difference being that terms related to $\cos^2 k_z$ also come into play, resulting in a stronger suppression of $|\Delta|$. This last case is illustrated by the dash-dotted curve in Fig. 1.

B. Critical SOIs

In this section, we examine the dependence of the magnitude of the gap function on the strength of SOI. As noted in Sec. IV, the effects of Rashba and Dresselhaus SOIs on the gap function are analogous, so we focus on the dependence of $|\Delta|$ on α . To this end, we integrate Eq. (31) with respect to k_z . This can be performed numerically for cases where $J \neq 0$, $\alpha \neq 0$, and $\beta \neq 0$. In the case where $J = 0.4\Delta_0$ and $\beta = 0.8\sqrt{\Delta_0/m}$, these results are illustrated by the solid curve in Fig. 2. It is evident from Fig. 2 that SOIs suppresses $|\Delta|$. Moreover, Fig. 2 also indicates that there is a critical value of SOI. If any SOI reaches or exceeds this value, the superconducting phase disappears. By comparing the solid curve with the dashed curve, which represents the case where $J = 0.4\Delta_0$ and $\beta = 0$, we observe that the critical value of one SOI

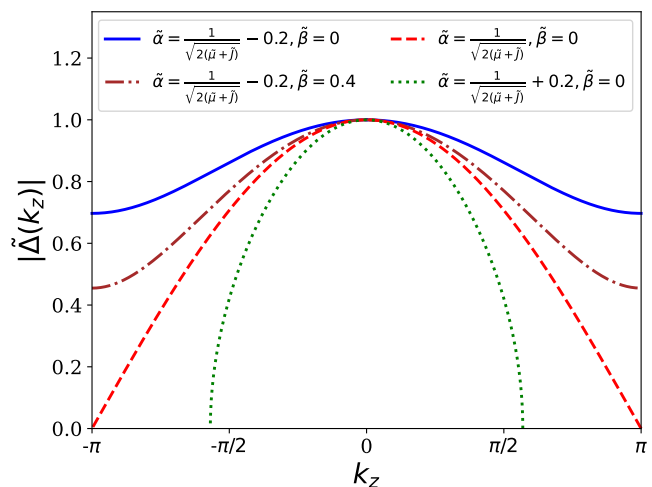


FIG. 1. Variation of the magnitude of the gap function with k_z momentum along the z direction. Calculations for all curves are performed with $\tilde{\mu} = \tilde{J} = 0.5$.

is unaffected by the presence of the other SOI. Therefore, the critical value for α calculated in Eq. (31) for the case $\beta = 0$ will also be valid for $\beta \neq 0$. To calculate this value, assume $\beta = 0$ in the integral in Eq. (31)

$$1 = -\frac{|\lambda|\rho_0^{2D}}{2} \int_{-\pi}^{\pi} \frac{dk_z}{2\pi} \ln \left(\frac{|\Delta|^2 + 2m(\mu - J\cos k_z)\alpha^2}{4\omega_D^2} \right). \quad (34)$$

To find the integral with respect to k_z in Eq. (34), we can follow a method very similar to the one shown in Appendix C. As a result, we obtain the following expression

$$1 = -|\lambda|\rho_0^{2D} \times \ln \left(\frac{\sqrt{|\Delta|^2 + 2m(\mu+J)\alpha^2} + \sqrt{|\Delta|^2 + 2m(\mu-J)\alpha^2}}{4\omega_D} \right). \quad (35)$$

From this, we find that the square of the magnitude of the gap function is

$$|\Delta|^2 = \Delta_0^2 - 2m\mu\alpha^2 + \frac{(mJ\alpha^2)^2}{\Delta_0^2}. \quad (36)$$

At zero temperature, the critical value of α at which the superconducting phase vanishes in the system described

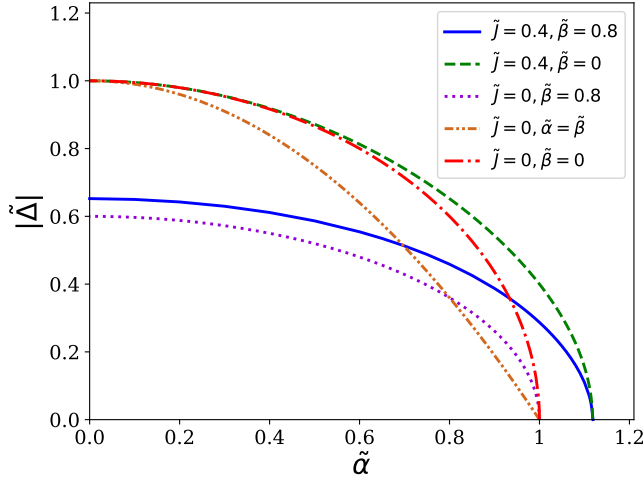


FIG. 2. Variation of the magnitude of the gap function with the strength of spin-orbit interaction at zero temperature. Calculations for all curves are performed with $\tilde{\mu} = 0.5$.

by the Hamiltonian (1) can be determined from Eq. (36) as follows

$$\alpha_C^J = \frac{\Delta_0}{J} \sqrt{\frac{\mu}{m} \left(1 - \sqrt{1 - \frac{J^2}{\mu^2}} \right)}. \quad (37)$$

As shown in Eq. (37), the critical value of the SOI depends on J . Generally, as J increases, this critical value also increases. This is because, as noted for Fig. 1, an increase in J leads to a rise in $|\Delta|$, necessitating a stronger SOI to nullify it. This behavior is also evident from the comparison of $J = 0$ and $J \neq 0$ cases, where $J = 0$ represents the scenario of pure $2D$ superconductors in the presence of Rashba and Dresselhaus SOIs. For $J = 0$, $\alpha \neq 0$, and $\beta \neq 0$, the solution to Eq. (31) can be obtained by setting $J = 0$ in Eq. (32)

$$|\Delta|^2 = \Delta_0^2 - 2m\mu(\alpha^2 + \beta^2) + \frac{4m^2\mu^2\alpha^2\beta^2}{\Delta_0^2}. \quad (38)$$

Note that Eq. (38) simplifies to the following form when $\alpha = \beta$

$$|\Delta| = \Delta_0 - \frac{2m\mu\alpha^2}{\Delta_0}. \quad (39)$$

From Eq. (38), we can determine the critical SOI value for pure $2D$ superconductors

$$\alpha_C^{2D} = \frac{\Delta_0}{\sqrt{2m\mu}}. \quad (40)$$

As seen in Fig. 2, the critical SOI value for the $J = 0$ curves is smaller compared to the case where $J \neq 0$. Generally, for the same value of μ

$$\alpha_C^J > \alpha_C^{2D}. \quad (41)$$

It should be noted that, in Fig. 2, with $\tilde{\mu} = 0.5$, the critical SOI value $\tilde{\alpha}_C^{2D}$ is 1.

VI. FINITE TEMPERATURE RESULTS

In this section, we examine how the magnitude of $|\Delta|$ and the critical temperature T_C change in the presence of Rashba and Dresselhaus SOIs at finite temperatures. To do this, we first express Eq. (26) at finite temperatures by converting to polar coordinates in \mathbf{k} -space. We then obtain the following equation

$$1 = \frac{|\lambda|\rho_0^{2D}}{2} \int_{-\pi}^{\pi} \frac{dk_z}{2\pi} \int_{-\pi}^{\pi} \frac{d\theta}{2\pi} \int_{-\omega_D}^{\omega_D} d\epsilon \frac{\tanh\left(\frac{\sqrt{\epsilon^2 + 2\eta_1\epsilon + \eta_2}}{2T}\right)}{\sqrt{\epsilon^2 + 2\eta_1\epsilon + \eta_2}}. \quad (42)$$

By writing

$$\tanh\left(\frac{\sqrt{\epsilon^2 + 2\eta_1\epsilon + \eta_2}}{2T}\right) = 1 - \frac{2}{1 + e^{\frac{\sqrt{\epsilon^2 + 2\eta_1\epsilon + \eta_2}}{T}}}, \quad (43)$$

we can see that if we study the temperature dependence of $\Delta(T)$, then we have to keep at $T \ll T_C$ the approximate $e^{-\frac{\sqrt{\epsilon^2 + 2\eta_1\epsilon + \eta_2}}{T}}$ dependence which is responsible for the T -dependence of $|\Delta|$. On the other hand, if we seek an equation for T_C , we neglect this term. Below, we examine these two cases separately.

A. The gap function at temperatures $T \ll T_C$

By substituting Eq. (43) into Eq. (42), we obtain two integrals. The first integral is identical to the one on the right-hand side of Eq. (27) and, as a result, is equal to the right-hand side of Eq. (31), with the only difference being that Δ is now a function of T . The second integral is given by the following expression

$$I(T) = -|\lambda|\rho_0^{2D} \int_{-\pi}^{\pi} \frac{dk_z}{2\pi} \int_{-\pi}^{\pi} \frac{d\theta}{2\pi} \int_{-\omega_D}^{\omega_D} d\epsilon \times \frac{\sum_{n=1}^{\infty} (-1)^{n+1} e^{-n\frac{\sqrt{\epsilon^2 + 2\eta_1\epsilon + \eta_2}}{T}}}{\sqrt{\epsilon^2 + 2\eta_1\epsilon + \eta_2}}. \quad (44)$$

where we used the following expansion for the small exponential term

$$(1 + e^x)^{-1} = \sum_{n=1}^{\infty} (-1)^{n+1} e^{-nx}. \quad (45)$$

From the integral representation of the modified Bessel function of the second kind [49] we can write

$$K_0\left(\frac{n\sqrt{\eta_2 - \eta_1^2}}{T}\right) = \frac{1}{2} \int_{-\infty}^{\infty} d\epsilon \frac{e^{-\frac{n}{2}\sqrt{\epsilon^2 + 2\eta_1\epsilon + \eta_2}}}{\sqrt{\epsilon^2 + 2\eta_1\epsilon + \eta_2}}. \quad (46)$$

On the other hand, we can represent the modified Bessel function of the second kind using the following series

$$K_0(x) = \sqrt{\frac{\pi}{2x}} e^{-x} \sum_{k=0}^{n-1} \frac{1}{(2x)^k} \frac{\Gamma(\frac{1}{2} + k)}{k! \Gamma(\frac{1}{2} - k)}. \quad (47)$$

Since $\frac{n\sqrt{\eta_2 - \eta_1^2}}{T} \gg 1$ in the case where $T \ll T_C$, we can approximate the series expansion given by Eq. (47) using only the first two terms. Then

$$\sum_{n=1}^{\infty} (-1)^{n+1} K_0 \left(\frac{n\sqrt{\eta_2 - \eta_1^2}}{T} \right) \approx \sqrt{\frac{\pi T}{2\sqrt{\eta_2 - \eta_1^2}}} e^{-\frac{\sqrt{\eta_2 - \eta_1^2}}{T}} \times \left(1 - \frac{T}{8\sqrt{\eta_2 - \eta_1^2}} \right). \quad (48)$$

Thus, by approximating $\pm\omega_D \rightarrow \pm\infty$ and substituting Eq. (48) in Eq. (44), we can obtain Eq. (42) as follows

$$1 = -\frac{|\lambda|\rho_0^{2D}}{2} \int_{-\pi}^{\pi} \frac{dk_z}{2\pi} \int_{-\pi}^{\pi} \frac{d\theta}{2\pi} \left\{ \ln \left(\frac{\eta_3 + \eta_4 \sin 2\theta}{4\omega_D^2} \right) + 4\sqrt{\frac{\pi T}{2\sqrt{\eta_2 - \eta_1^2}}} e^{-\frac{\sqrt{\eta_2 - \eta_1^2}}{T}} \left(1 - \frac{T}{8\sqrt{\eta_2 - \eta_1^2}} \right) \right\}. \quad (49)$$

Eq. (49) represents the gap equation for layered superconductors in the presence of Rashba and Dresselhaus SOIs at finite temperatures where $T \ll T_C$. One significant conclusion from this equation is that, similar to zero temperature, the effect of tunneling of electrons between layers on the intralayer gap is significant in the presence of SOIs at temperatures below the critical temperature. In other words, the anisotropy of the gap function at finite temperatures is also due to the presence of SOIs.

Eq. (49) can be solved numerically. Fig. 3 illustrates the dependence of $|\Delta|$ on α at temperatures $T = 0, 0.05\Delta_0$, and $0.1\Delta_0$ with $J = 0.4\Delta_0$ and $\beta = 0.3\sqrt{\Delta_0/m}$. Fig. 3 shows that temperature, in conjunction with SOIs, suppresses $|\Delta|$. Another result indicated by this figure is that the critical SOI value decreases as the temperature increases.

B. Critical temperature

The critical temperature can be determined using Eq. (42), where the only difference is that we assume $\Delta = 0$ in the expression for η_2 . By performing tedious but straightforward calculations, we obtain the following equation for the critical temperature

$$1 = \frac{|\lambda|\rho_0^{2D}}{2} \int_{-\pi}^{\pi} \frac{dk_z}{2\pi} \int_{-\pi}^{\pi} \frac{d\theta}{2\pi} \left(2 \ln \left(\frac{2\omega_D e^\gamma}{\pi T_C} \right) - \sqrt{\tilde{\eta}_2 - \eta_1^2} \right), \quad (50)$$

where $\tilde{\eta}_2 = J^2 \cos^2 k_z + 2m\mu(\alpha^2 + \beta^2 + 2\alpha\beta \sin 2\theta)$, and γ is the Euler-Mascheroni constant. As seen from Eq. (50), the contribution of J to T_C is only possible in the presence of SOIs. By numerically solving Eq. (50), we can determine the critical temperature for layered superconductors in the presence of Rashba and Dresselhaus

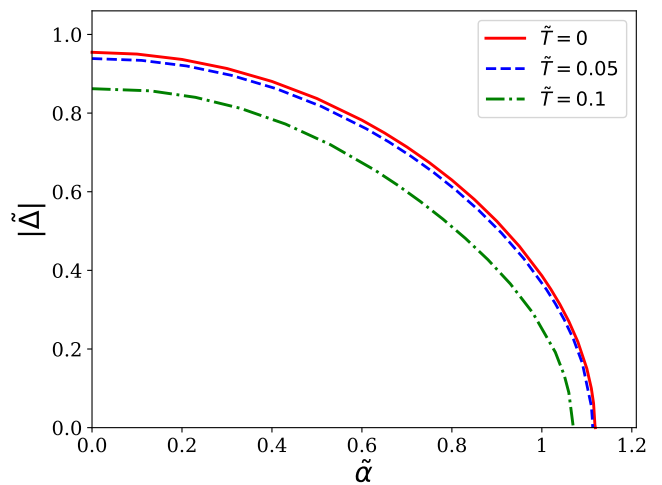


FIG. 3. Variation of the magnitude of the gap function with the strength of spin-orbit interaction at temperatures $T \ll T_C$. Calculations for all curves are performed with $\tilde{J} = 0.4, \tilde{\beta} = 0.3$, and $\tilde{\mu} = 0.5$.

TABLE I. BCS equation for layered superconductors in the presence of Rashba and Dresselhaus SOIs. In these calculations, $\tilde{\mu} = 0.5$ has been chosen.

$\tilde{\alpha}$	$\tilde{\beta}$	\tilde{J}	T_C/Δ_0
0	0	0	0.567
0.2	0	0	0.514
0.2	0.2	0	0.502
0.2	0.2	0.2	0.503
0.4	0	0	0.472
0.4	0.2	0	0.471
0.4	0.2	0.2	0.472
0.4	0.4	0	0.468
0.4	0.4	0.2	0.469
0.4	0.4	0.4	0.471

SOIs. These results are presented in Table I. As can be seen from this table, the influence of Rashba and Dresselhaus SOIs on the BCS equation is substantial. Generally, SOIs reduce the ratio T_C/Δ_0 . The presence of a single SOI causes the most significant suppression, while the presence of a second SOI also leads to suppression, but to a lesser extent. Large values of J slightly increase the T_C/Δ_0 ratio.

VII. CONCLUSIONS

In this study we have extended the theory of layered superconductors with intralayer pairing interaction to include Rashba and Dresselhaus SOIs. One of the key results we obtained is that the presence of SOIs renders the gap function anisotropic in these systems. This ef-

fect is demonstrated in Eq. (32) for zero temperature and in Eq. (49) for finite temperatures. Generally, our work serves as a foundational theory for experimental studies such as [26–31]. Moreover, the anisotropy introduced by SOIs could be crucial in understanding superconductivity and its anisotropic behavior across various systems. For instance, anisotropic 2D superconductivity has been observed in $\text{KTaO}_3(111)$ interfaces, with critical temperatures dependent on orientation and sensitivity to bias direction, though the underlying mechanisms are not yet fully understood [51, 52]. Notably, Rashba-type spin splitting has been reported for the $\text{KTaO}_3(111)$ surface [53]. However, this work has not explained the highly anisotropic nature of superconductivity. Our study, in contrast, demonstrates that additional anisotropy may exist in superconductors as a result of Rashba-type spin splitting.

Another important result of our study is the existence of a critical value for the SOIs, where, when one of the SOIs reaches this value, the superconducting phase in the system ceases. We calculated these values analytically for zero temperature, as provided in Eq. (37). For

finite temperatures, the critical values are determined by the numerical solution of Eq. (49) (see Fig. 3). This result indicates that, similar to the Pauli limit, the model exhibits a Rashba and/or Dresselhaus limit in which the paired states will be disrupted. Therefore, in experimental studies, it is necessary to consider that the superconducting phase could be terminated due to the effects of the SOIs.

ACKNOWLEDGMENTS

BT is supported by the Turkish Academy of Sciences (TUBA).

Appendix A: Components of the Green's function in the presence of SOIs

If we substitute Eqs. (13a) and (13b) into the equations of motion (9) and (10), we find the following equations

$$(i\omega_n - \xi_{\mathbf{k}k_z} - \lambda G^{\downarrow\downarrow}(0+)) G^{\uparrow\uparrow}(\mathbf{k}, k_z, \omega_n) + (\alpha(k_y + ik_x) + \beta(k_x + ik_y) + \lambda G^{\uparrow\downarrow}(0+)) G^{\downarrow\uparrow}(\mathbf{k}, k_z, \omega_n) - \lambda F^{\uparrow\downarrow}(0+) F^{\downarrow\uparrow}(\mathbf{k}, k_z, \omega_n) = 1, \quad (\text{A1a})$$

$$(i\omega_n - \xi_{\mathbf{k}k_z} - \lambda G^{\downarrow\downarrow}(0+)) G^{\uparrow\downarrow}(\mathbf{k}, k_z, \omega_n) + (\alpha(k_y + ik_x) + \beta(k_x + ik_y) + \lambda G^{\uparrow\downarrow}(0+)) G^{\downarrow\downarrow}(\mathbf{k}, k_z, \omega_n) = 0, \quad (\text{A1b})$$

$$(i\omega_n - \xi_{\mathbf{k}k_z} - \lambda G^{\uparrow\uparrow}(0+)) G^{\downarrow\uparrow}(\mathbf{k}, k_z, \omega_n) + (\alpha(k_y - ik_x) + \beta(k_x - ik_y) + \lambda G^{\downarrow\uparrow}(0+)) G^{\uparrow\uparrow}(\mathbf{k}, k_z, \omega_n) = 0, \quad (\text{A1c})$$

$$(i\omega_n - \xi_{\mathbf{k}k_z} - \lambda G^{\uparrow\uparrow}(0+)) G^{\downarrow\downarrow}(\mathbf{k}, k_z, \omega_n) + (\alpha(k_y - ik_x) + \beta(k_x - ik_y) + \lambda G^{\downarrow\uparrow}(0+)) G^{\uparrow\downarrow}(\mathbf{k}, k_z, \omega_n) - \lambda F^{\downarrow\uparrow}(0+) F^{\uparrow\downarrow}(\mathbf{k}, k_z, \omega_n) = 1, \quad (\text{A1d})$$

$$(-i\omega_n - \xi_{\mathbf{k}k_z} - \lambda G^{\downarrow\downarrow}(0+)) F^{\uparrow\downarrow}(\mathbf{k}, k_z, \omega_n) + \lambda F^{\uparrow\uparrow\downarrow}(0+) G^{\downarrow\downarrow}(\mathbf{k}, k_z, \omega_n) = 0, \quad (\text{A1e})$$

$$(-i\omega_n - \xi_{\mathbf{k}k_z} - \lambda G^{\uparrow\uparrow}(0+)) F^{\downarrow\uparrow}(\mathbf{k}, k_z, \omega_n) + \lambda F^{\downarrow\downarrow\uparrow}(0+) G^{\uparrow\uparrow}(\mathbf{k}, k_z, \omega_n) = 0, \quad (\text{A1f})$$

where $\xi_{\mathbf{k}k_z}$ is determined by Eq. (15b). We note that when evaluating Eqs. (A1e) and (A1f), we take into account

$$\sum_{\gamma} \left\{ \alpha \left((\sigma_x)_{a\gamma} p_y - (\sigma_y)_{a\gamma} p_x \right) + \beta \left((\sigma_x)_{a\gamma} p_x - (\sigma_y)_{a\gamma} p_y \right) \right\} F_{jj'}^{\uparrow\gamma b}(\mathbf{r}, \tau; \mathbf{r}', \tau') = 0. \quad (\text{A2})$$

in Eq. (10). To understand the reason behind Eq. (A2), we begin by assuming spin state a is up (\uparrow). Consequently, this leads to spin state b being down (\downarrow) in Eq. (10). Therefore, for the left-hand side of Eq. (A2) to be non-zero, γ must be \uparrow . However, both σ_x and σ_y matrices have zero elements for $\uparrow\uparrow$, indicating the validity of Eq. (A2). A similar situation can be observed for $a = \downarrow$ and $b = \uparrow$.

To find the analytical expressions for the Green's functions from Eqs. (A1a) – (A1f), we first determine the functions $G^{\downarrow\uparrow}(\mathbf{k}, k_z, \omega_n)$ and $F^{\uparrow\downarrow}(\mathbf{k}, k_z, \omega_n)$ from Eqs. (A1c) and (A1f). Subsequently, by writing them in Eq. (A1a), we can derive the following equation for $G^{\uparrow\uparrow}(\mathbf{k}, k_z, \omega_n)$

$$\left(i\omega_n - \xi_{\mathbf{k}k_z} - \frac{(\alpha^2 + \beta^2)(k_x^2 + k_y^2) + 4\alpha\beta k_x k_y}{i\omega_n - \xi_{\mathbf{k}k_z}} + \frac{|\Delta|^2}{-i\omega_n - \xi_{\mathbf{k}k_z}} \right) \times G^{\uparrow\uparrow}(\mathbf{k}, k_z, \omega_n) = 1, \quad (\text{A3})$$

where $|\Delta|^2$ is determined by Eq. (16). Similarly, by determining the functions $G^{\uparrow\downarrow}(\mathbf{k}, k_z, \omega_n)$ and $F^{\downarrow\uparrow}(\mathbf{k}, k_z, \omega_n)$ from Eqs. (A1b) and (A1e), and then writing them in Eq. (A1d), we obtain the same equation for $G^{\downarrow\downarrow}(\mathbf{k}, k_z, \omega_n)$ as in Eq. (A3). From this, we establish that $G^{\uparrow\uparrow}(\mathbf{k}, k_z, \omega_n) = G^{\downarrow\downarrow}(\mathbf{k}, k_z, \omega_n)$, and from Eq. (A3), we find Eq. (14a). Here, note that in Eq. (A3), we do not account for the contributions of the $\lambda G^{\uparrow\uparrow, \downarrow\downarrow}(0+)$ terms, as done in the theory of pure superconductors without SOIs [47]. This is because these terms only add to the chemical potential and hence are of no interest. Additionally, in deriving Eq. (A3), we also neglect the contributions of $\lambda G^{\uparrow\downarrow, \downarrow\uparrow}(0+)$ terms because these contributions are very small, on the order of λ/μ . Thus, by obtaining the analytical expressions represented by Eq. (14a) for $G^{\uparrow\uparrow, \downarrow\downarrow}(\mathbf{k}, k_z, \omega_n)$, we find Eq. (14b) for the off-diagonal

elements of the normal Green's function from Eqs. (A1b) and (A1c), and Eq. (14c) for the anomalous Green's functions from Eqs. (A1e) and (A1f).

Appendix B: Contribution of Integral I_1

In this appendix, we examine the contribution of the I_1 integral to Δ . In other words, we assume the gap equation to be of the form

$$1 = I_0 + I_1, \quad (\text{B1})$$

where the calculations related to I_0 have been carried out in Secs. V and VI, and

$$I_1 = -|\lambda|T \sum_n \int_{-\pi}^{\pi} \frac{dk_z}{2\pi} \int_{-\infty}^{\infty} \frac{d^2k}{(2\pi)^2} \frac{1}{\omega_n^2 + \xi_{\mathbf{k}k_z}^2 + |\Delta|^2 + \xi_{SO}^2} \times \frac{1}{(\omega_n^2 + \xi_{\mathbf{k}k_z}^2) \frac{\omega_n^2 + \xi_{\mathbf{k}k_z}^2 + |\Delta|^2 + \xi_{SO}^2}{2\xi_{SO}^2 \xi_{\mathbf{k}k_z}^2}}. \quad (\text{B2})$$

In order to begin, we perform the summation over n for the integral I_1 . Since the poles of the integrand are $z_{1,2} = \pm i\sqrt{\xi_{\mathbf{k}k_z}^2 + |\Delta|^2 + \xi_{SO}^2}/2\pi T$ and $z_{3,4} = \pm i\frac{\xi_{\mathbf{k}k_z}}{2\pi T}$, where $z = n + 1/2$, we find that

$$I_1 = \frac{|\lambda|}{2} \int_{-\pi}^{\pi} \frac{dk_z}{2\pi} \int_{-\infty}^{\infty} \frac{d^2k}{(2\pi)^2} \frac{\xi_{SO}^2 \xi_{\mathbf{k}k_z}}{(2\pi T)^4} \left[\frac{(2\pi T)^4 \tanh\left(\frac{\xi_{\mathbf{k}k_z}}{2T}\right)}{(|\Delta|^2 + \xi_{SO}^2)^2} - i \left(\frac{1}{(z_1 - z_3)^2} - \frac{1}{(z_1 - z_4)^2} + \frac{2}{(z_1 - z_2)(z_1 - z_3)} \right. \right. \\ \left. \left. - \frac{2}{(z_1 - z_2)(z_1 - z_4)} \right) \frac{\tan(\pi z_1)}{(z_1 - z_2)^2} + 2i \left(\frac{1}{z_2 - z_3} - \frac{1}{z_2 - z_4} \right) \frac{\tan(\pi z_2)}{(z_1 - z_2)^3} + i\pi \left(\frac{1}{(z_1 - z_3)(z_2 - z_3)^2} - \frac{1}{(z_1 - z_4)(z_2 - z_4)^2} \right) \right. \\ \left. \times \frac{\tan(\pi z_2)}{(z_1 - z_2)^4 \cos^2(\pi z_1)} + i\pi \left(\frac{1}{z_2 - z_3} - \frac{1}{z_2 - z_4} \right) \frac{1}{(z_1 - z_2)^2 \cos^2(\pi z_2)} \right]. \quad (\text{B3})$$

In Eq. (B3), we can see how much more complicated the I_1 integral is compared to I_0 . Note that the I_0 integral is computed as shown in Eq. (26) using similar steps.

Since finite temperatures suppress Δ , the largest contribution of I_1 to Δ occurs at $T = 0$. Therefore, we continue our analysis for $T = 0$. In this case, using Eqs. (26) and (B3), we can write Eq. (B1) as follows

$$1 = \frac{|\lambda|\rho_0^{2D}}{2} \int_{-\pi}^{\pi} \frac{dk_z}{2\pi} \int_{-\pi}^{\pi} \frac{d\theta}{2\pi} \int_{-\omega_D}^{\omega_D} d\epsilon \left[\frac{3}{\sqrt{\epsilon^2 + 2\eta_1\epsilon + \eta_2}} + \frac{2}{\epsilon \cdot \eta_1 + \eta_2} \left(2 \left(\epsilon - \sqrt{\epsilon^2 + 2\eta_1\epsilon + \eta_2} \right) \right. \right. \\ \left. \left. + \frac{2|\Delta|^2(\sqrt{\epsilon^2 + 2\eta_1\epsilon + \eta_2} - 1)}{\epsilon \cdot \eta_1 + \eta_2} - \frac{|\Delta|^2}{\sqrt{\epsilon^2 + 2\eta_1\epsilon + \eta_2}} \right) \right], \quad (\text{B4})$$

where ϵ and $\eta_{1,2}$ are defined by Eqs. (28a) – (28c). By performing the integration with respect to ϵ in Eq. (B4), we find that

$$1 = -\frac{|\lambda|\rho_0^{2D}}{4} \int_{-\pi}^{\pi} \frac{dk_z}{2\pi} \int_{-\pi}^{\pi} \frac{d\theta}{2\pi} \left[\ln \left(\frac{\eta_3 + \eta_4 \sin 2\theta}{4\omega_D^2} \right) + \ln \left(\frac{\eta_3 - \eta_4 \sin 2\theta}{4\omega_D^2} \right) - 4\omega_D^2 \left(\frac{1}{\eta_3 + \eta_4 \sin 2\theta} \right. \right. \\ \left. \left. \times \left(\frac{|\Delta|^2}{\eta_3 + \eta_4 \sin 2\theta} - 1 \right) + \frac{1}{\eta_3 - \eta_4 \sin 2\theta} \right. \right. \\ \left. \left. \times \left(\frac{|\Delta|^2}{\eta_3 - \eta_4 \sin 2\theta} - 1 \right) \right]. \quad (\text{B5})$$

From Eq. (B5), we see that even when the integral I_1 is present, the contribution of J to Δ at $T = 0$ only occurs in the presence of SOI. Finally, using the integrals from

Appendix C and $\int_{-\pi}^{\pi} dx (a+b \sin x)^{-2} = 2\pi a(a^2-b^2)^{-3/2}$, we find that

$$1 = -|\lambda|\rho_0^{2D} \int_{-\pi}^{\pi} \frac{dk_z}{2\pi} \left[\ln \left(\frac{\sqrt{|\Delta|^2 + 2m(\mu - J \cos k_z)(\alpha + \beta)^2} + \sqrt{|\Delta|^2 + 2m(\mu - J \cos k_z)(\alpha - \beta)^2}}{4\omega_D} \right) - 2\omega_D^2 \frac{|\Delta|^2 (|\Delta|^2 + 2m(\mu - J \cos k_z)(\alpha^2 + \beta^2)) - (|\Delta|^2 + 2m(\mu - J \cos k_z)(\alpha^2 - \beta^2))^2 + 16m^2\mu^2\alpha^2\beta^2}{(|\Delta|^2 + 2m(\mu - J \cos k_z)(\alpha + \beta)^2)^{\frac{3}{2}} (|\Delta|^2 + 2m(\mu - J \cos k_z)(\alpha - \beta)^2)^{\frac{3}{2}}} \right] \quad (\text{B6})$$

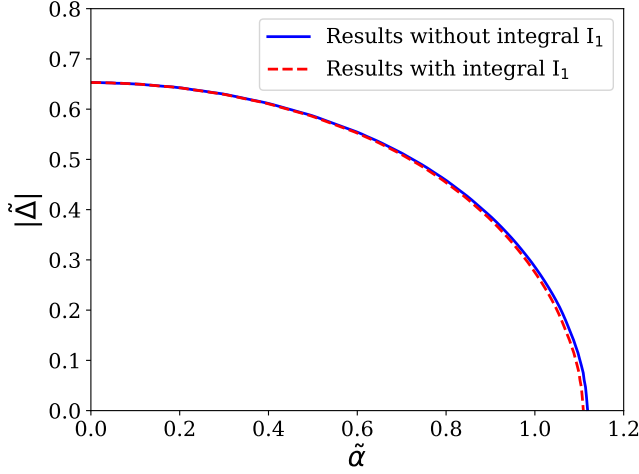


FIG. 4. The contribution of the I_1 integral, determined using Eq. (B2), to the gap equation. The calculations are performed with the values $\tilde{\mu} = 0.5$, $\tilde{\omega}_D = 0.05$, $\tilde{J} = 0.4$, and $\tilde{\beta} = 0.8$.

From Eq. (B6), it is evident that the contribution of the I_1 integral to the gap equation calculated using Eq. (B1) is a term multiplied by ω_D^2 . In all practical cases, since the cutoff energy ω_D is much smaller than μ ($\omega_D \ll \mu$), this contribution is considered to be very small. This can also be seen from Fig. 4. In this figure, the solid line represents the gap equation calculated with $1 = I_0$ using Eq. (31), while the dashed line represents the gap equation calculated with $1 = I_0 + I_1$ using Eq. (B6). As shown, the contribution of the I_1 integral to $|\Delta|$ is very small. The presence of I_1 only results in a very slight reduction in the critical value due to SOIs.

Appendix C: Integration with respect to the polar angle

In Eq. (29), the integral with respect to the polar angle is given by $\int_{-\pi}^{\pi} d\theta \ln(\eta_3 + \eta_4 \sin 2\theta)$, where η_3 and η_4 are expressed in Eqs. (30a) and (30b), respectively. To evaluate this integral, we first make the substitution

$\varphi = 2\theta - \frac{3\pi}{2}$, and then substitute $z = \tan \varphi$,

$$\int_{-\pi}^{\pi} d\theta \ln(\eta_3 + \eta_4 \sin 2\theta) = \int_{-\infty}^{\infty} \frac{dz}{1+z^2} \times \ln \left(\frac{\eta_3^2 - \eta_4^2 + \eta_3^2 z^2}{1+z^2} \right). \quad (\text{C1})$$

To evaluate the integral in Eq. (C1), we consider the complex integral $\oint_C \frac{dz}{1+z^2} \ln(i\sqrt{\eta_3^2 - \eta_4^2} + \eta_3 z)$. As shown in Fig. 5, we choose an analytical function in the upper half-plane. Then

$$\begin{aligned} \oint_C \frac{dz}{1+z^2} \ln(i\sqrt{\eta_3^2 - \eta_4^2} + \eta_3 z) &= 2\pi i \\ &\times \lim_{z \rightarrow i} \frac{\ln(i\sqrt{\eta_3^2 - \eta_4^2} + \eta_3 z)}{z+i} \\ &= \pi \ln(\eta_3 + \sqrt{\eta_3^2 - \eta_4^2}) + \frac{i}{2}\pi^2. \end{aligned} \quad (\text{C2})$$

On the other hand, for the contour shown in Fig. 5, we can write

$$\begin{aligned} \oint_C \frac{dz}{1+z^2} \ln(i\sqrt{\eta_3^2 - \eta_4^2} + \eta_3 z) &= \int_{-R}^R \frac{dz}{1+z^2} \ln(i\sqrt{\eta_3^2 - \eta_4^2} + \eta_3 z) \\ &+ \int_{\Gamma} \frac{dz}{1+z^2} \ln(i\sqrt{\eta_3^2 - \eta_4^2} + \eta_3 z), \end{aligned} \quad (\text{C3})$$

where the integral along Γ on the right-hand side is zero. At the same time,

$$\begin{aligned} \int_{-R}^R \frac{dz}{1+z^2} \ln(i\sqrt{\eta_3^2 - \eta_4^2} + \eta_3 z) &= \int_0^R \frac{dz}{1+z^2} \ln(\eta_3^2 - \eta_4^2 + \eta_3^2 z) \\ &+ \int_0^R \frac{dz}{1+z^2} i\pi \end{aligned} \quad (\text{C4})$$

holds. Using Eqs. (C3) and (C4), we find from Eq. (C2) that

$$\int_{-\infty}^{\infty} \frac{dz}{1+z^2} \ln(\eta_3^2 - \eta_4^2 + \eta_3^2 z) = 2\pi \ln(\eta_3 + \sqrt{\eta_3^2 - \eta_4^2}). \quad (\text{C5})$$

Thus, for the integration with respect to the polar angle in the gap equation at $T = 0$, we find that

$$\int_{-\pi}^{\pi} d\theta \ln(\eta_3 + \eta_4 \sin 2\theta) = 2\pi \ln \left(\frac{\eta_3 + \sqrt{\eta_3^2 - \eta_4^2}}{2} \right). \quad (\text{C6})$$

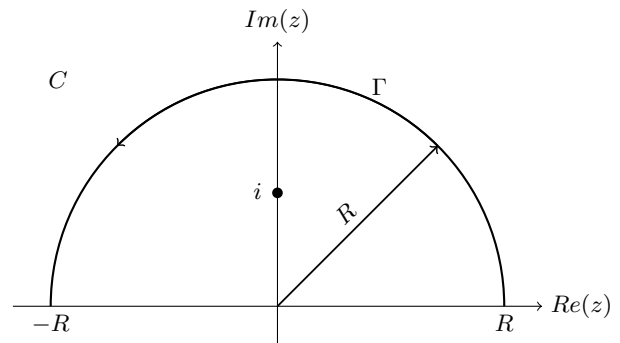


FIG. 5. Semicircular contour for integral (C2).

-
- [1] J. B. Miller, D. M. Zumbühl, C. M. Marcus, Y. B. Lyanda-Geller, D. Goldhaber-Gordon, K. Campman, and A. C. Gossard, Gate-Controlled Spin-Orbit Quantum Interference Effects in Lateral Transport, *Phys. Rev. Lett.* **90**, 076807 (2003).
- [2] L. Meier, G. Salis, I. Shorubalko, E. Gini, S. Schön, and K. Ensslin, Measurement of Rashba and Dresselhaus spin-orbit magnetic fields, *Nature Physics* **3**, 650 (2007).
- [3] A. Manchon, H. C. Koo, J. Nitta, S. M. Frolov, and R. A. Duine, New perspectives for Rashba spin-orbit coupling, *Nature Materials* **14**, 871 (2015).
- [4] D. Bercioux and P. Lucignano, Quantum transport in Rashba spin-orbit materials: a review, *Reports on Progress in Physics* **78**, 106001 (2015).
- [5] G. Bihlmayer, P. Noel, D. V. Vyalikh, E. V. Chulkov, and A. Manchon, Rashba-like physics in condensed matter, *Nature Reviews Physics* **4**, 642 (2022).
- [6] M. Hoesch, M. Muntwiler, V. N. Petrov, M. Hengsberger, L. Patthey, M. Shi, M. Falub, T. Greber, and J. Osterwalder, Spin structure of the Shockley surface state on Au(111), *Phys. Rev. B* **69**, 241401 (2004).
- [7] M. Mende, K. Ali, G. Poelchen, S. Schulz, V. Mandic, A. V. Tarasov, C. Polley, A. Generalov, A. V. Fedorov, M. Güttler, C. Laubschat, K. Kliemt, Y. M. Koroteev, E. V. Chulkov, K. Kummer, C. Krellner, D. Y. Usachov, and D. V. Vyalikh, Strong Rashba Effect and Different f-d Hybridization Phenomena at the Surface of the Heavy-Fermion Superconductor CeIrIn₅, *Advanced Electronic Materials* **8**, 2100768 (2022).
- [8] G. Dresselhaus, Spin-Orbit Coupling Effects in Zinc Blende Structures, *Phys. Rev.* **100**, 580 (1955).
- [9] M. C. Lüffe, J. Kailasvuori, and T. S. Nunner, Relaxation mechanisms of the persistent spin helix, *Phys. Rev. B* **84**, 075326 (2011).
- [10] C. Autieri, P. Barone, J. Ślawińska, and S. Picozzi, Persistent spin helix in Rashba-Dresselhaus ferroelectric CsBiNb₂O₇, *Phys. Rev. Mater.* **3**, 084416 (2019).
- [11] X.-Z. Lu and J. M. Rondinelli, Strain engineering a persistent spin helix with infinite spin lifetime, *Phys. Rev. B* **107**, 035155 (2023).
- [12] Q. Wang, K. Kalantar-Zadeh, A. Kis, J. N. Coleman, and M. S. Strano, Electronics and optoelectronics of two-dimensional transition metal dichalcogenides, *Nature Nanotechnology* **7**, 699 (2012).
- [13] M. Shimozawa, S. K. Goh, R. Endo, R. Kobayashi, T. Watashige, Y. Mizukami, H. Ikeda, H. Shishido, Y. Yanase, T. Terashima, T. Shibauchi, and Y. Matsuda, Controllable Rashba Spin-Orbit Interaction in Artificially Engineered Superlattices Involving the Heavy-Fermion Superconductor CeCoIn₅, *Phys. Rev. Lett.* **112**, 156404 (2014).
- [14] M. Sato and Y. Ando, Topological superconductors: a review, *Reports on Progress in Physics* **80**, 076501 (2017).
- [15] M. M. Sharma, P. Sharma, N. K. Karn, and V. P. S. Awana, Comprehensive review on topological superconducting materials and interfaces, *Superconductor Science and Technology* **35**, 083003 (2022).
- [16] M. Schlipf and F. Giustino, Dynamic Rashba-Dresselhaus Effect, *Phys. Rev. Lett.* **127**, 237601 (2021).
- [17] M. Sato, Y. Takahashi, and S. Fujimoto, Non-Abelian Topological Order in s-Wave Superfluids of Ultracold Fermionic Atoms, *Phys. Rev. Lett.* **103**, 020401 (2009).
- [18] J. D. Sau, R. M. Lutchyn, S. Tewari, and S. Das Sarma, Generic New Platform for Topological Quantum Computation Using Semiconductor Heterostructures, *Phys. Rev. Lett.* **104**, 040502 (2010).
- [19] Y. Volpez, D. Loss, and J. Klinovaja, Rashba sandwiches with topological superconducting phases, *Phys. Rev. B* **97**, 195421 (2018).
- [20] V. Mourik, K. Zuo, S. M. Frolov, S. R. Plissard, E. P. A. M. Bakkers, and L. P. Kouwenhoven, Signatures of Majorana Fermions in Hybrid Superconductor-Semiconductor Nanowire Devices, *Science* **336**, 1003 (2012).
- [21] M. T. Deng, C. L. Yu, G. Y. Huang, M. Larsson, P. Caroff, and H. Q. Xu, Anomalous Zero-Bias Conductance Peak in a Nb-InSb Nanowire-Nb Hybrid Device, *Nano Lett.* **12**, 6414 (2012).
- [22] H. Pan and S. Das Sarma, Physical mechanisms for zero-bias conductance peaks in Majorana nanowires, *Phys. Rev. Res.* **2**, 013377 (2020).
- [23] R. S. Deacon, J. Wiedenmann, E. Bocquillon, F. Domínguez, T. M. Klapwijk, P. Leubner, C. Brüne, E. M. Hankiewicz, S. Tarucha, K. Ishibashi, H. Buhmann, and L. W. Molenkamp, Josephson Radiation from Gapless Andreev Bound States in HgTe-Based Topolog-

- ical Junctions, *Phys. Rev. X* **7**, 021011 (2017).
- [24] S. M. Albrecht, A. P. Higginbotham, M. Madsen, F. Kuemmeth, T. S. Jespersen, J. Nygard, P. Krogstrup, and C. M. Marcus, Exponential protection of zero modes in Majorana islands, *Nature* **531**, 206 (2016).
- [25] S. Nadj-Perge, I. K. Drozdov, J. Li, H. Chen, S. Jeon, J. Seo, A. H. MacDonald, B. A. Bernevig, and A. Yazdani, Observation of majorana fermions in ferromagnetic atomic chains on a superconductor, *Science* **346**, 602 (2014).
- [26] S. Yoshizawa, T. Kobayashi, Y. Nakata, K. Yaji, K. Yokota, F. Komori, S. Shin, K. Sakamoto, and T. Uchihashi, Atomic-layer Rashba-type superconductor protected by dynamic spin-momentum locking, *Nature Communications* **12**, 1462 (2021).
- [27] T. Uchihashi, Surface atomic-layer superconductors with Rashba/Zeeman-type spin-orbit coupling, *AAPPS Bulletin* **31**, 27 (2021).
- [28] H. Ryu, J.-M. Lihm, J. Cha, B. Kim, B. S. Kim, W. Kyung, I. Song, Y. Kim, G. Han, J. Denlinger, I. Chung, C.-H. Park, S. R. Park, and C. Kim, Chemical control of the Rashba spin splitting size of α -GeTe(111) surface states by adjusting the potential at the topmost atomic layer, *Phys. Rev. B* **103**, 245113 (2021).
- [29] K. Sakamoto, T. Kobayashi, K. Yaji, T. Shishidou, and M. Donath, Spin-polarized electrons in atomic layer materials formed on solid surfaces, *Progress in Surface Science* **97**, 100665 (2022).
- [30] K. Yaji, Y. Ohtsubo, S. Hatta, H. Okuyama, K. Miyamoto, T. Okuda, A. Kimura, H. Namatame, M. Taniguchi, and T. Aruga, Large Rashba spin splitting of a metallic surface-state band on a semiconductor surface, *Nature Communications* **1**, 17 (2010).
- [31] A. V. Matetskiy, S. Ichinokura, L. V. Bondarenko, A. Y. Tupchaya, D. V. Gruznev, A. V. Zotov, A. A. Saranin, R. Hobara, A. Takayama, and S. Hasegawa, Two-Dimensional Superconductor with a Giant Rashba Effect: One-Atom-Layer Tl-Pb Compound on Si(111), *Phys. Rev. Lett.* **115**, 147003 (2015).
- [32] R. Masutomi, T. Okamoto, and Y. Yanase, Unconventional superconducting phases in multilayer films with layer-dependent Rashba spin-orbit interactions, *Phys. Rev. B* **101**, 184502 (2020).
- [33] L. Bulaevskii, Inhomogeneous state and the anisotropy of the upper critical field in layered superconductors with Josephson layer interaction, *Zh. Eksp. Teor. Fiz* **65**, 1278 (1973).
- [34] R. A. Klemm, A. Luther, and M. R. Beasley, Theory of the upper critical field in layered superconductors, *Phys. Rev. B* **12**, 877 (1975).
- [35] Z. Gulácsi, M. Gulácsi, and I. Pop, Enhancement of the superconducting critical temperature in layered compounds, *Phys. Rev. B* **37**, 2247 (1988).
- [36] T. Schneider, H. De Raedt, and M. Frick, On the theory of layered high-temperature superconductors, *Zeitschrift für Physik B Condensed Matter* **76**, 10.1007/BF01323482 (1989).
- [37] E. P. Nakhmedov and E. V. Tahirov, Josephson-coupled layered superconductors with two order parameters. I. Upper critical magnetic field, *Journal of Physics: Condensed Matter* **6**, 2245 (1994).
- [38] R. Wesche, *High-Temperature Superconductors* (Springer Nature Switzerland, 2025) pp. XVII, 173.
- [39] M. Gurvitch, J. M. Valles, A. M. Cucolo, R. C. Dynes, J. P. Garno, L. F. Schneemeyer, and J. V. Waszczak, Reproducible tunneling data on chemically etched single crystals of YBa₂Cu₃O₇, *Phys. Rev. Lett.* **63**, 1008 (1989).
- [40] T. Ekino and J. Akimitsu, Energy gaps in Bi-Sr-Ca-Cu-O and Bi-Sr-Cu-O systems by electron tunneling, *Phys. Rev. B* **40**, 6902 (1989).
- [41] K. F. McCarty, J. Z. Liu, R. N. Shelton, and H. B. Radousky, Electronic Raman scattering of YBa₂Cu₃O₇ using c-axis polarization: Evidence for two characteristic superconducting energies, *Phys. Rev. B* **42**, 9973 (1990).
- [42] J. Takada, T. Terashima, Y. Bando, H. Mazaki, K. Iijima, K. Yamamoto, and K. Hirata, Quasiparticle density of states in the perpendicular direction to the Cu-O planes in YBa₂Cu₃O_{7-x} single-crystal thin films, *Phys. Rev. B* **40**, 4478 (1989).
- [43] Z.-X. Shen, D. S. Dessau, B. O. Wells, D. M. King, W. E. Spicer, A. J. Arko, D. Marshall, L. W. Lombardo, A. Kapitulnik, P. Dickinson, S. Doniach, J. DiCarlo, T. Loeser, and C. H. Park, Anomalously large gap anisotropy in the a-b plane of Bi₂Sr₂CaCu₂O_{8+ δ} , *Phys. Rev. Lett.* **70**, 1553 (1993).
- [44] D. N. Basov and T. Timusk, Electrodynamics of high-*T_c* superconductors, *Rev. Mod. Phys.* **77**, 721 (2005).
- [45] O. Fischer, M. Kugler, I. Maggio-Aprile, C. Berthod, and C. Renner, Scanning tunneling spectroscopy of high-temperature superconductors, *Rev. Mod. Phys.* **79**, 353 (2007).
- [46] M. Smidman, O. Stockert, E. M. Nica, Y. Liu, H. Yuan, Q. Si, and F. Steglich, Colloquium: Unconventional fully gapped superconductivity in the heavy-fermion metal CeCu₂Si₂, *Rev. Mod. Phys.* **95**, 031002 (2023).
- [47] A. A. Abrikosov, L. P. Gorkov, and I. E. Dzyaloshinski, *Methods of quantum field theory in statistical physics* (Courier Corporation, 2012).
- [48] J. Schliemann and D. Loss, Anisotropic transport in a two-dimensional electron gas in the presence of spin-orbit coupling, *Phys. Rev. B* **68**, 165311 (2003).
- [49] G. B. Arfken, H. J. Weber, and F. E. Harris, *Mathematical Methods for Physicists (Seventh Edition)* (Academic Press, Boston, 2013).
- [50] S. H. Liu and R. A. Klemm, Intralayer versus interlayer pairing in the copper oxide superconductors: The three- and four-layer problems, *Phys. Rev. B* **45**, 415 (1992).
- [51] C. Liu, X. Yan, D. Jin, Y. Ma, H.-W. Hsiao, Y. Lin, T. M. Bretz-Sullivan, X. Zhou, J. Pearson, B. Fisher, J. S. Jiang, W. Han, J.-M. Zuo, J. Wen, D. D. Fong, J. Sun, H. Zhou, and A. Bhattacharya, Two-dimensional superconductivity and anisotropic transport at KTaO₃(111) interfaces, *Science* **371**, 716 (2021).
- [52] E. G. Arnault, A. H. Al-Tawhid, S. Salmani-Rezaie, D. A. Muller, D. P. Kumah, M. S. Bahramy, G. Finkelstein, and K. Ahadi, Anisotropic superconductivity at KTaO₃(111) interfaces, *Science Advances* **9**, eadf1414 (2023).
- [53] F. Y. Bruno, S. McKeown Walker, S. Riccò, A. de la Torre, Z. Wang, A. Tamai, T. K. Kim, M. Hoesch, M. S. Bahramy, and F. Baumberger, Band Structure and Spin-Orbital Texture of the (111)-KTaO₃ 2D Electron Gas, *Advanced Electronic Materials* **5**, 1800860 (2019).